PROCEEDINGS A

rspa.royalsocietypublishing.org

Research

Article submitted to journal

Stabilizing a homoclinic stripe

Theodore Kolokolnikov[1], Michael Ward[2], Justin Tzou[3] and Juncheng Wei[2]

[1] Department of Mathematics and Statistics, Dalhousie University, Halifax, Canada

[2] Department of Mathematics , University of British Columbia,

[3] Department of Mathematics, Macquarie University

For a large class of reaction-diffusion systems with large diffusivity ratio, it is well known that a two-dimensional stripe (whose cross-section is a one-dimensional homoclinic spike) is unstable and breaks up into spots. Here, we study two effects that can stabilize such a homoclinic stripe. First, we consider the addition of anisotropy to the model. For the Schnakenberg model, we show that (an infinite) stripe can be stabilized if the fast-diffusing variable (substrate) is sufficiently anisotropic. Two types of instability thresholds are derived: zigzag (or bending) and breakup instabilities. The instability boundaries subdivide parameter space into three distinct zones: stable stripe, unstable stripe due to bending, and unstable due to breakup instability. Numerical experiments indicate that the breakup instability is supercritical leading to a "spotted-stripe" solution. Finally, we perform a similar analysis for the Klausmeyer model of vegetation patterns on a steep hill, and examine transition from spots to stripes.

THE ROYAL SOCIETY PUBLISHING

Introduction

Consider a typical Reaction-diffusion model, such as the Schnakenberg model, which admits a one-dimensional spike solution corresponding to a homoclinic orbit of the underlying slow-diffusing variable. When such one-dimensional spike is extended trivially to the second dimension, the result is what we shall call a "homoclinic stripe". In common situations, it is well-established that a "homoclinic stripe" is *unstable* and breaks up into spots, unless a domain is very "thin" [1–4]. This breakup is illustrated in Figures 1 row B and figure 2 row 1. In this paper we examine two situations that can potentially stabilize a homoclinic stripe: adding anisotripy or drift to the fast-diffusing variable. We show that a sufficient amount of anisotropy or drift can stabilize a homoclinic stripe of *any* length.

For concreteness, we concentrate on the well-studied Schnakenberg model [5–7] and its variants, but we anticipate these techniques can be extended to other settings. We first examine the anisotropic version of Schankenberg model, using the following scaling in two dimensions:

$$\begin{cases} u_t = \varepsilon^2 \left(u_{xx} + u_{yy}\right) - u + u^2 v, \\ 0 = d^2 v_{xx} + b^2 v_{yy} + A - \dfrac{u^2 v}{\varepsilon} \end{cases} , \quad x \in (-L, L), \quad y \in \mathbb{R}. \tag{0.1}$$

We will assume Neumann boundary conditions in the x direction, with the stripe extending to infinity in the y-direction ($y \in \mathbb{R}$), which is the most potentially destabilizing case anyway, although our results generalize easily to the case of finite stripe.

We further assume that $\varepsilon \ll O(1)$ and $d \gg O(\sqrt{\varepsilon})$, whereas A and L are $O(1)$. In this case, u and v become weakly coupled and the one-dimensional spike solution to (0.1) is asymptotically close to a sech^2-type profile.

Equations (0.1) model the following process: a fast-diffusing substrate v is consumed by a slowly diffusing activator u, which decays with time. The substrate is being pumped into the system at rate A. The reaction kinetics for u and v occur at different scales: u reacts much slower than v, so that v is effectively slave to u. Note that we scaled the system so that the activator u diffuses isotropically; the anisotropy is only present in the substrate (the case of anisotropic diffusion in u can be reduced to (0.1) by scaling the y coordinate appropriately).

Figure 1 illustrates our results. For sufficiently small b, the stripe is fully stable (row A). As b is increased, there are two types of instabilities that appear, depending on how large d is. These instabilities are triggered by either large ($O(1)$) or small ($O(\varepsilon^2)$) eigenvalues, and are illustrated in rows B and C, respectively. We will refer to them as *breakup* and *zigzag* instabilities, respectively. As shown in the figure, the two instability boundaries (indicated by red and blue curves) *cross* each-other. The crossing point is shown in green. The main result of this paper is to characterize this crossing analytically.

We now summarize the main result as follows. Consider the *stripe solution*, where $u(x, y, t)$ is localized along a vertical line. Such a solution is shown row A (last snapshot) and has the asymptotic profile $u(x, y, t) \sim \frac{LA}{2} \operatorname{sech}^2\left(\frac{x}{2\varepsilon}\right)$ (see below for derivation). The stripe is *stable* provided that $b < \min(b_1, b_2)$, where $b = b_1$ and $b = b_2$ are thresholds for breakup and zigzag instabilities, respectively. The stripe is *unstable* when $b > \min(b_1, b_2)$. Refer to Figure 1 (top).

Suppose further that

$$\sqrt{\varepsilon} \ll d \ll 1. \tag{0.2}$$

Then the asymptotics for stability boundaries b_1 and b_2 have explicit asymptoics

$$b_1 \sim 1.0127\ LA\frac{\varepsilon}{d}; \tag{0.3}$$

$$b_2 \sim 2.5152\ \frac{d^2}{\sqrt{L}A}. \tag{0.4}$$

Breakup instabilities occur when $b > b_1$. Zigzag instabilities happen when $b > b_2$ (the formula (0.4) is actually valid for any $d \gg \sqrt{\varepsilon}$, whereas formula (0.3) requires further restriction $\sqrt{\varepsilon} \ll d \ll 1$).

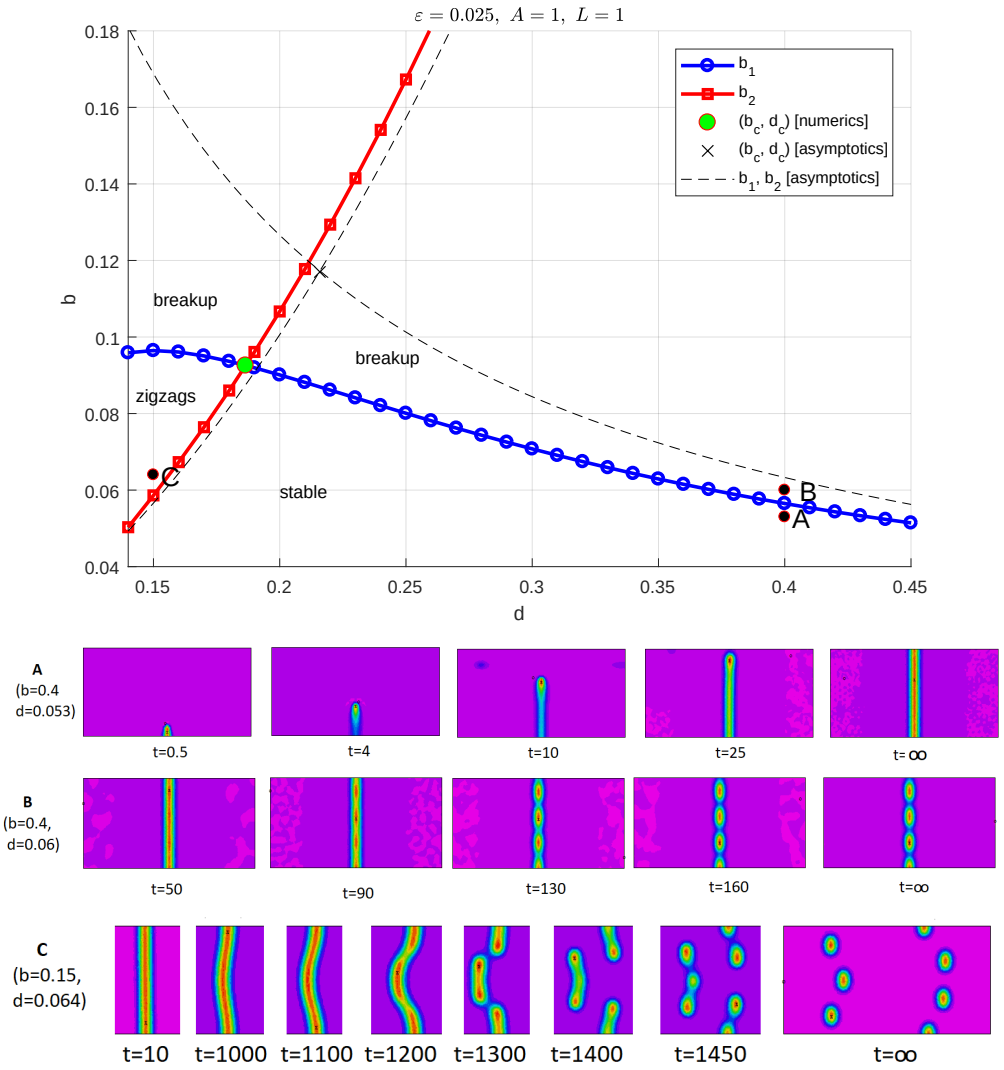

Figure 1: Top: Boundaries for zigag and breakup instabilities in the $d-b$ parameter plane with $\varepsilon = 0.025,\ (x,y) \in [-1,1] \times [0,1],\ A = 1$. Note a good agreement between asymptotics and numerics. Rows A-C show snapshots of full numerical simulations of (0.1) in different parameter regions. Parameters A are in the stable region. Parameters B: stripe exhibits a breakup instability. Parameter C: The stripe is stable with respect to breakup instability, but unstable with respect to a zigzag instability. As a result, the stripe starts to bend (note the slow time scale). Eventually, this is followed by a breakup of a bended stripe.

As Figure 1 shows, the two stability boundaries intersect. Let (d_c, b_c) be the point in (d,b) space at which $b_1 = b_2$. From (0.3), (0.4), this point is asymptotically given by:

$$d_c \sim 0.7384 L^{1/2} A^{2/3} \varepsilon^{1/3}; \quad b_c \sim 1.371 L^{1/2} A^{1/3} \varepsilon^{2/3}. \tag{0.5}$$

If $d > d_c$ then breakup instabilities occur as b is increased above b_1. If $\varepsilon^{1/2} \ll d < d_c$, then zigzag instabilities occur as b is increased above b_2.

Note that there is a relatively large error in (d_c, b_c) when $\varepsilon = 0.05$. This is due to $O(\varepsilon^{1/3})$ scaling in (0.5). The following table shows the error behaviour as is halfed. It shows that the relative error does indeed decrease as $\varepsilon \to 0$.

	Numerics		Asymptotcs		Rel.err	
ε	d_c	b_c	d_c	b_c	$\frac{d_c-d}{d_c}$	$\frac{b_c-b}{b_c}$
0.05	0.2201	0.1375	0.2720	0.1861	19.1%	26%
0.025	0.18648	0.09255	0.2159	0.1172	13.6%	21%
0.0125	0.1536	0.06102	0.1714	0.0738	10.3%	17%

Stripe steady state.

We begin by constructing a stripe steady state. Such a solution independent of y or t, so that (0.1) reduce to

$$0 = \varepsilon^2 u_{xx} - u + u^2 v, \quad 0 = d^2 v_{xx} + A - \frac{u^2 v}{\varepsilon}, \quad x \in (-L, L) \tag{0.6}$$

with Neumann boundary condtions $u_x(\pm L) = v_x(\pm L) = 0$. The asymptotic construction of a spike profile to (0.6) is by now very standard (see e.g. [7,8]) but we briefly review it here for completeness and to settle the notation. We assume the spike has a maximum at $x = 0$. In the inner region we scale $u(x) = U(z), \quad v(x) = V(z)$, which yields

$$U_{zz} - U + U^2 V = 0; \quad d^2 V_{zz} = \varepsilon U^2 V - \varepsilon^2 A. \tag{0.7}$$

Assume that

$$d^2 \gg O(\varepsilon) \tag{0.8}$$

Then to leading order we have $V_{zz} \sim 0$ so that V is a constant: $V \sim v_0$. Then to leading order, U satisfies $U \sim w/v_0$ where w is the ground state satisfying

$$w_{zz} - w + w^2 = 0. \tag{0.9}$$

with a well-known explicit solution given by $w(z) = \frac{3}{2}\operatorname{sech}^2(z/2)$. It remains to determine v_0. To do so, we integrate the second equation in (0.6) which yields

$$v_0 \sim \frac{3}{LA} \tag{0.10}$$

where we used the fact that $\int_{-\infty}^{\infty} w^2(z)dz = 6$. In conclusion, we obtained:

$$u \sim \frac{LA}{2}\operatorname{sech}^2\left(\frac{x}{2\varepsilon}\right); \quad v(0) \sim \frac{3}{LA}. \tag{0.11}$$

Stability: large eigenvalues.

We linearize the stripe using

$$u(x, y, t) = u(x) + e^{\lambda t} e^{imy} \phi(x)$$
$$v(x, y, t) = v(x) + e^{\lambda t} e^{imy} \phi(x)$$

which results in the following one-dimensional eigenvalue problem,

$$\left(\lambda + \varepsilon^2 m^2\right) \phi = \varepsilon^2 \phi_{xx} - \phi + 2uv\phi + u^2 \psi; \tag{0.12a}$$

$$0 = d^2 \psi_{xx} - b^2 m^2 \psi - 2\frac{uv\phi}{\varepsilon} - \frac{u^2 \psi}{\varepsilon}, \tag{0.12b}$$

with Neumann boundary conditions $\phi'(\pm L) = \psi'(\pm L) = 0$.

In the inner region $x = \varepsilon z$, to leading order, (0.12*a*) can be written as

$$\left(\lambda+\varepsilon^2 m^2\right)\phi = L_0\phi + w^2 v_0^{-2}\psi_0 \tag{0.13}$$

where

$$L_0\phi := \phi_{zz} - \phi + 2w\phi \tag{0.14}$$

is the local linear operator of the associated ground state $w(z)$, and $\psi_0 = \psi(0)$. To determine ψ_0, we approximate $-2\frac{uv\phi}{\varepsilon} - \frac{u^2\psi}{\varepsilon} \sim \left(-\int_{-\infty}^{\infty} 2w\phi dz - \psi_0 v_0^{-2}\int_{-\infty}^{\infty} w^2 dz\right)\delta(x)$ so that

$$\psi(x) \sim \left(-\int_{-\infty}^{\infty} 2w\phi dz - \psi_0 v_0^{-2}\int_{-\infty}^{\infty} w^2 dz\right) G(x) \tag{0.15}$$

where G satisfies

$$d^2 G_{xx} - m^2 b^2 G + \delta(x) = 0, \quad G'(\pm L) = 0. \tag{0.16}$$

The solution to (0.16) is given by

$$G = \frac{1}{2dmb\sinh\left(\frac{mb}{d}L\right)}\cosh\left(\frac{mb}{d}(|x|-L)\right)$$

and in particular,

$$G(0) = \frac{1}{2dmb}\coth\left(\frac{mb}{d}L\right).$$

Upon plugging in $x=0$ into (0.15) we obtain

$$v_0^{-2}\psi_0 = \frac{-\int 2w\phi}{\int w^2 + \frac{v_0^2}{G(0)}}.$$

Now consider the critical scaling

$$m = \hat{m}\varepsilon^{-1}; \quad b = \hat{b}\varepsilon$$

so that (0.13) becomes

$$\left(\lambda+\hat{m}^2\right)\phi = L_0\phi - \chi\left(\int w^2\phi\right)w^2 \quad \text{where } \chi = \frac{1}{3 + v_0^2 d\hat{m}\hat{b}\tanh\left(\frac{\hat{m}\hat{b}}{d}L\right)}. \tag{0.17}$$

where we used $\int w^2 = 6$. Problem (0.17) is equivalent to solving

$$f(\lambda+\hat{m}^2) = 3 + \frac{9d\hat{b}}{(LA)^2}\hat{m}\tanh\left(\frac{\hat{b}L}{d}\hat{m}\right) \tag{0.18}$$

where

$$f(\mu) := \int w(L_0-\mu)^{-1}w^2. \tag{0.19}$$

The function $f(\mu)$ can be expressed in terms of hypergeometric functions – see e.g. [9]. However the resulting expression is unwieldy and at the end still needs to be evaluated numerically. Here we compute $f(\mu)$ directly by solving numerically the associated BVP $(L_0-\mu)\phi = w^2$ and

integrating numerically. The graph of $f(\mu)$ is as follows:

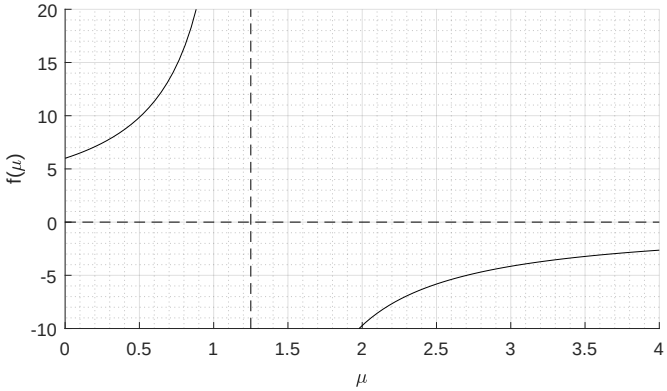

(0.20)

The vertical asymptote corresponds to the eigenvalue $\mu = 5/4$ of the local operator L_0, and asymptotic expansion near $\mu = 5/4$ shows that f blows up to the left of this asymptote, in agreement with the graph (0.20). Moreover, $f(0) = \int w^2 = 6$.

Simple sketching show that there is always an instability band when $\hat{b}$ is sufficiently large, and there is full stability when $\hat{b}$ is sufficiently small. The instability threshold happens when there is a double root for the equation

$$f(\hat{m}^2) = 3 + 9\alpha\hat{m}\tanh(\beta\hat{m}) \text{ where } \alpha = \frac{d\hat{b}}{(LA)^2}, \quad \beta = \frac{\hat{b}L}{d}. \tag{0.21}$$

The following table gives the double-root boundary for selected values of β.

$\beta = \frac{\hat{b}L}{d}$	$\alpha = \frac{d\hat{b}}{(LA)^2}$	$\alpha\beta (= \frac{\hat{b}^2}{LA^2})$	$\alpha/\beta (= \frac{d^2}{L^3A^2})$
0.05	30.416	1.5208	608.319
0.1	15.2277	1.52277	152.277
0.2	7.65315	1.53063	38.2658
0.5	3.16896	1.58448	6.33792
1	1.76	1.76	1.76
1.4	1.40648	1.96907	1.00463
2	1.17	2.35	0.588
4	0.998	4	0.249
8	0.975	7.8	0.121

Of particular interest are the following limits:

- d small: In this limit, $\beta \to \infty$ so that $\tanh$ in (0.21) can be replaced by 1, and the instability threshold corresponds to the double-root of the equation $f(\hat{m}^2) = 3 + 9\alpha\hat{m}$, which numerically yields $\alpha \sim 0.975$ as $\beta \to \infty$. In the original variables, this yields the threshold (0.3).
- d large: then $\beta \to 0$ and the instability threshold corresponds to the double-root of the equation $f(\hat{m}^2) = 3 + 9\alpha\beta\hat{m}^2$, which numerically yields $\alpha\beta \sim 1.5208$ as $\beta \to 0$. In the original variables, this yields the threshold

$$b_1 \sim 1.233AL^{1/2}\varepsilon, \quad \text{when } d \gg O(1). \tag{0.22}$$

We will come back to (0.22) in the context of incorporating large drift, see below.

Small eigenvalues.

Small eigenvalues arise from the translation invariance of the inner problem for the spike [8]. They correspond to an odd solution of the linearized equation (0.12). To leading order in ε, the eigenvalue is zero and a higher-order expansion is necessary to resolve the stability. Proceeding as in [3], we therefore expand both the steady state and the eigenfunction in the inner region using the stretched variable $z = x/\varepsilon$:

$$x = \varepsilon z, \quad u(x) = U(z), \quad v(x) = V(z), \quad \psi(x) = \Psi(z), \quad \phi(x) = \Phi(z).$$

The resulting equations are:

$$U_{zz} - U + U^2 V = 0, \qquad V_{zz} = \frac{\varepsilon}{d^2}\left(U^2 V - \varepsilon A\right); \tag{0.23}$$

$$(\lambda + \varepsilon^2 m^2)\Phi = \Phi_{zz} - \Phi + 2UV\Phi + U^2\Psi. \tag{0.24}$$

$$d^2\Psi_{zz} = mb^2\varepsilon^2\Psi + 2UV\Phi\varepsilon + U^2\Psi\varepsilon, \tag{0.25}$$

To leading order in ε, the solution to (0.24) is given by $\Phi \sim U_y$, $\lambda = 0$.To resolve the next order, we start by multipying (0.24) by U_z and integrating to obtain

$$\left(m\varepsilon^2 + \lambda\right)\int \Phi U_z = \int U^2\left(U_z\Psi - V_z\Phi\right). \tag{0.26}$$

Estimating $\Phi \sim U_y$ and integrating the right hand side by parts yields

$$\left(m\varepsilon^2 + \lambda\right)\int U_z^2 \sim \int \frac{U^3}{3}\left(V_{zz} - \Psi_z\right) \tag{0.27}$$

and using (0.23) we further estimate

$$\int \frac{U^3}{3} V_{zz} \sim \int \left(\frac{\varepsilon}{3d^2}U^5 V - \frac{\varepsilon^2}{3d^2}AU^3\right).$$

Finally from (0.25) we estimate

$$d^2\Psi_{zz} \sim 2UV\Phi\varepsilon \sim \left(U^2\right)_z V_0\varepsilon$$

so that

$$\Psi_z \sim U^2 V_0 \frac{\varepsilon}{d^2} + \Psi_z(\infty) \tag{0.28}$$

and (0.28) becomes

$$\left(m\varepsilon^2 + \lambda\right)\int U_z^2 \sim -\int \frac{U^3}{3}\left(\frac{\varepsilon^2}{d^2}A + \Psi_z(\infty)\right). \tag{0.29}$$

Next we compute the outer solution to and match $\Psi_z(\infty)$.In the outer variables we get

$$\Psi_z(\infty) = \varepsilon\psi_x\left(0^+\right).$$

Recall that ψ satisfies (0.12*b*). The last two terms decay exponentially and are taken are zero, so that

$$\psi(x) \sim C\cosh\left(\frac{bm}{d}(x - L)\right), \quad x > 0$$

To get C, multiply by x and integrate, assuming that Φ, Ψ is odd to get

$$-d^2\left(\psi(0^+) - \psi(0^-)\right) - \int 2UVU_z\varepsilon z dz = 0$$

$$2d^2\psi\left(0^+\right) = -v_0^{-1}\varepsilon\int\left(w^2\right)_z z dz = v_0^{-1}\varepsilon\int w^2$$

so that

$$C = \frac{\varepsilon v_0^{-1}\int w^2}{2d^2}\frac{1}{\cosh\left(\frac{bm}{d}L\right)}.$$

and finally

$$\Psi_z(\infty) = \varepsilon\psi_x\left(0^+\right) \sim -\varepsilon^2 v_0^{-1}\frac{bm}{2d^3}\tanh\left(\frac{bm}{d}L\right)\int w^2. \tag{0.30}$$

Upon substiting (0.30) into (0.29) we obtain, after some algebra,

$$\lambda + \varepsilon^2 m^2 \sim -\frac{2}{3}\frac{LA^2}{d^2}\left(1 - L\frac{bm}{d}\tanh\left(\frac{bm}{d}L\right)\right)\varepsilon^2 \tag{0.31}$$

where we used: $\int w^2 = 6, \int w_z^2 = \frac{6}{5}, \int w^3 = \frac{36}{5}$, $v_0^{-1} = LA/3$.

Rewrite (0.31) as

$$\hat{\lambda} \sim -1 + \hat{m}\tanh(\hat{m}) - \alpha\hat{m}^2 \tag{0.32}$$

where

$$\alpha = \frac{3}{2}\frac{d^4}{LA^2b^2}, \quad \hat{\lambda} = \frac{\lambda}{\varepsilon^2}\frac{3}{2}\frac{d^2}{LA^2}, \quad \hat{m} = mLb/d. \tag{0.33}$$

From (0.32), there is a double root when $\alpha = 0.23716$ corresponding to $\hat{m} = 2.26488$. Instability exists when $\alpha > 0.23716$, or $b > b_2$, where b_2 is given by (0.4).

This concludes the derivation of (0.3) and (0.4).

Vegetation patterns on a sloping ground.

Finally, we extend this analysis to a variant of the Schnakenberg model which incorporates the water flowing down the hill. The equations are

$$u_t = \varepsilon^2\left(u_{xx} + u_{yy}\right) - u + u^2 v, \tag{0.34a}$$

$$0 = d^2\left(v_{xx} + v_{yy}\right) + cv_x + A - \frac{u^2 v}{\varepsilon} \tag{0.34b}$$

For simplicity we will assume periodic boundary conditions in the x direction:

$$u(-L, y, t) = u(L, y, t); \quad v(-L, y, t) = v(L, y, t),$$

with the stripe extending to infinity in the y-direction ($y \in \mathbb{R}$). The main motivation for considering drift comes from the Klausmeyer vegetation model of localized patterns [10]. There, v represents water concentration in the soil whereas u is the plant density. In addition to the usual diffusion (assumed to be isotropic here for simplicity), the water flows down the slope. This is represented by the cv_x term (positive c assumes the water flows from right to left). In fact equations (0.34) are special case of Klausmeyer model when water evaporation is assumed small (water evaporation is modelled by adding $-ev$ term to the right hand side of (0.34*b*))

There are numerous papers studying the transition between homogeneous vegetation, vegetation spots and vegetation stripes. For an very incomplete list of references, see for example [4,11–16] and references therein. Generally speaking, spots transition to stripes, and stripes to uniform state, when precipitation rate A is increased.

Here, we show the transition of spots to stripes analytically in the regime of large slope gradient (represented by parameter c) and small diffusion d. The stripes extend in the y-direction, so that they are perpendicular to the slope. The existence of stable stripes for large c was observed numerically in [4,16], matching observations in nature [17,18]. By contrast, in [4] the authors show analytically that a stripe is unstable (in particular when the slope gradient is sufficiently small) and breaks up into spots.

Generally speaking, we find a spot-to-stripe transition as d is sufficiently decreased (and with c large). We restrict the analysis of (0.34) to the regime

$$d = O(\varepsilon); \quad c \gg 1. \tag{0.35}$$

With this restriction, the vegetation density has a sech^2-type profile in the x-direction, which we extend into a two-dimensional stripe. This makes it possible to determine the stability thresholds of the stripe analytically.

As shown in Appendix A, with restriction (0.35), the cross-section of the stripe has the spike profile has the form (0.11), except that x is replaced by $x - st$, where s is the (slow) speed of motion. This speed is easily computed using solvability condition (as was already done in [19], or see Appendix A) with the result that

$$s = \frac{8}{21} L^2 A^2 \frac{\varepsilon}{c}, \text{ when } c = O\left(\frac{1}{\varepsilon}\right). \tag{0.36}$$

Repeating the analysis for large eigenvalue yields the problem (0.17) but with

$$\chi = \frac{1}{3 + \hat{d}^2 \hat{m}^2 L v_0^2}.$$

As a consequence, the analysis leading to (0.22) applies, and it follows that stripe is **stable** provided $d < d_1$ where

$$d_1 \sim 1.233 A L^{1/2} \varepsilon, \quad \text{with } c \gg 1. \tag{0.37}$$

This threshold is illustrated in Figure 2. In the first two rows, $d > d_1$ and the stripe breaks up into spots, which then travel together forming a spotted-stripe pattern. In the second row, we took $d = 1.3 A L^{1/2} \varepsilon$. This is very close to the stable regime; the stripe still breaks up but not completely, indicating that the breakup instability is supercritical (i.e. reversible). For $d = 1.2 A L^{1/2} \varepsilon$ (so that $d = 0.97 d_1$, the stable side of the threshold), the stripe is seen to be stable. Stripe stability appears to be very robust: even initial conditions consisting of a single spot evolve into a stable stripe or spotted stripe as shown in rows (d,e), depending on whether $d < d_1$ or $d > d_1$.

Discussion.

For the Klausmeyer model, we have shown that adding sufficient anisotropy can lead to stable stripes. Unlike the previous works [1–4] which show that only a stripe of very small $O(\varepsilon)$ length can be stabilized in the isotropic case, here we show that the stripe of infinite length can become stable under sufficient anisotropy.

We also showed that the boundaries for zigzag and breakup instabilities cross when $d = d_c = O\left(\varepsilon^{1/3}\right)$, as b is increased. This analysis has similarities to the analysis of double-Hopf point of a spike in the Gray-Scott model – see for example [20–22] – although the resulting NLEP problem is has a somewhat different form, and it is enough to consider real solutions here (whereas full complex solutions arise when discussing a Hopf bifurcations). In these works, it is shown that a single spike in one dimension can become unstable due to either oscillations in position or in height, when the zero in the left hand side in (0.1) is replaced by τv_t and as τ is increased. These two instabilities also cross each-other when $A = O(\varepsilon^{1/6})$ (with $d = 1, b = 0$). We remark that this hopf-hopf crossing has been recently extendend to a two-dimensional spike in [23], where an unusual $\log\log\varepsilon$ scaling for the crossing point is derived.

An entirely different mechanism to stabilize a stripe is by adding saturation as described in [24]. Adding sufficient saturation can turn homoclinic (unstable) stripe into a heteroclinic (stable) stripe having a mesa-type profile consisting of back-to-back interfaces.

In the limit of large d (or equivalently, the limit of large c for the drift problem (0.34)), v only depends on y. We may integrate out the x-direction for (0.1) to obtain the following limiting

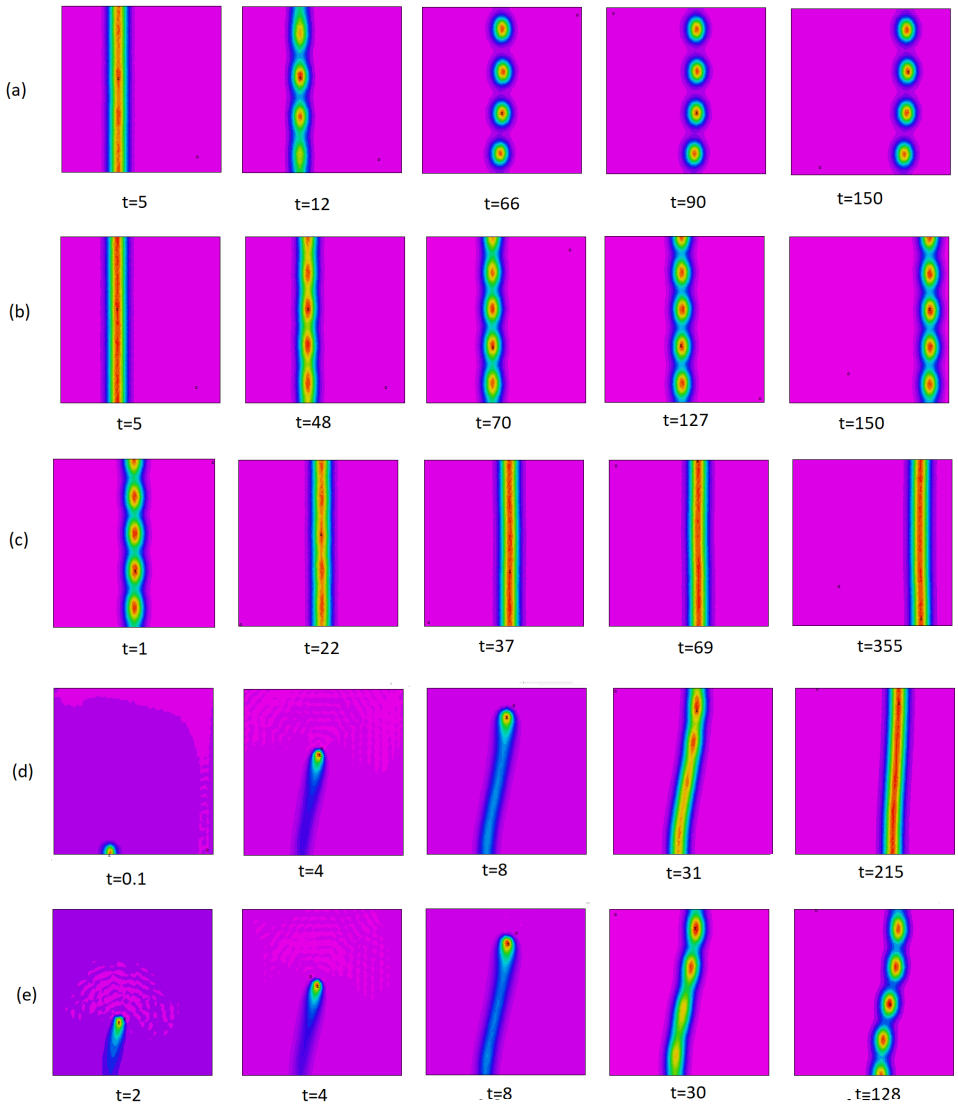

Figure 2: Simulation of (0.34) with $\varepsilon = 0.05$, $A = L = 1$, $c = 10$, and with d as follows: (a) $d = 1.8\varepsilon$; (b) $d = 1.3\varepsilon$; (c) $d = 1.2\varepsilon$; (d) $d = 1.2\varepsilon$; (e) $d = 1.3\varepsilon$. Initial conditions are close to those shown in the first column.

system

$$\begin{cases} u_t = \varepsilon^2 \left(u_{xx} + u_{yy}\right) - u + u^2 v, \\ 0 = b^2 v_{yy} + A - v(y) \int_{-L}^{L} \dfrac{u^2}{\varepsilon} dx \end{cases} , \quad x \in (-L, L), \quad y \in \mathbb{R}. \tag{0.38}$$

This is analogous to a so-called shadow limit, but in one direction only. In particular, the breakup instability threshold (0.22) can be derived directly from (0.38). It would be interesting to study spike dynamics for this system. The same system also arises in the limit of large drift $c \to \infty$ for (0.34).

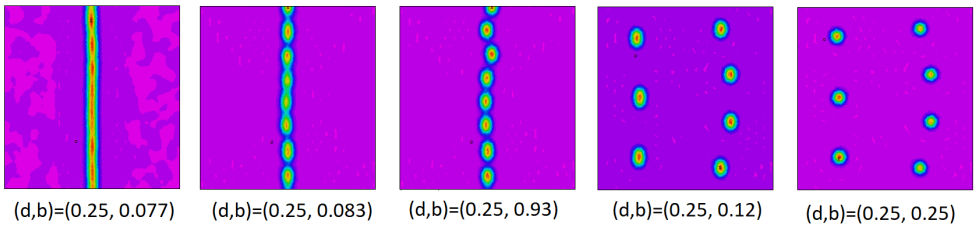

Figure 3: Simulation of (0.1) on a square 2x2 domain with $\varepsilon = 0.025$, $A = 1$ and with d and b as indicated. For each value of (d, b) the eventual steady state is shown (at $t = 10^7$). As anisotropy is decreased, first, the stripe bifurates into a spotted stripe, then the spotted stripe breaks up resulting in a more uniform spot distribution.

There are many open questions. For example, even when the stripe breaks up, the resulting spots can still align, forming a "spotted stripe". As the anisotropy is further decreased, the spotted stripe itself undergoes secondary bifurcation, eventually resulting in a more uniform spot distribution. This is illustrated in Figure 3. We plan to address this transition in future work.

APPENDIX: Speed of propagation

In this appendix we derive the formula (0.36) for the speed of propagation of a stripe. Similar formula was previously derived in [19]. Assuming stripe moves in the $x-$direction only, equations (0.34) reduce to

$$u_t = \varepsilon^2 u_{xx} - u + u^2 v, \;\; 0 = c v_x + A - \frac{u^2 v}{\varepsilon} \tag{0.39}$$

Assume that c scales like

$$c = \frac{c_0}{\varepsilon}$$

and expand

$$u(x,t) = U(z), \; v(x,t) = V(z), \quad z = \frac{x - s_0 \varepsilon^2 t}{\varepsilon}.$$

Then expand

$$U = U_0 + \varepsilon U_1, \quad V = V_0 + \varepsilon V_1 + \ldots, \;\; c = \frac{c_0}{\varepsilon}.$$

At the leading order, we obtain

$$U_{0zz} - U_0 + U_0^2 V_0 = 0, \quad V_{0z} = 0 \tag{0.40}$$

and the next order equations are

$$-s_0 U_{0z} = U_{1zz} - U_1 + 2U_0 V_0 U_1 + U_0^2 V_1; \quad V_{1z} = \frac{U_0^2 V_0}{c_0}. \tag{0.41}$$

Equation (0.40) yield

$$V_0 \equiv \text{const}; \;\; U_0 = w(z)/V_0$$

so that (0.41) simplifies to

$$-\frac{s}{V_0} w_z = U_{1zz} - U_1 + 2wU_1 + \frac{w^2}{V_0^2} V_1; \quad V_{1z} = \frac{w^2}{c_0 V_0}.$$

Multiplying the equation for U_1 by w_z and integrating then yields

$$-\frac{s_0}{V_0} \int_{-\infty}^{\infty} w_z^2 dz = \frac{1}{3V_0^2} \int_{-\infty}^{\infty} \left(w^3\right)_z V_1 dz = -\frac{1}{3c_0 V_0^3} \int_{-\infty}^{\infty} w^5 dz.$$

As before, to compute V_0 we integrate the equation for v in (0.39) using periodic boundary conditions to obtain

$$V_0 = \frac{\int w^2 dz}{2LA}$$

so that

$$s_0 = \frac{4L^2A^2}{3c_0\left(\int w^2 dz\right)^2}\frac{\int_{-\infty}^{\infty} w^5 dz}{\int_{-\infty}^{\infty} w_z^2 dz}$$

Finally, using $\int w^2 = 6,\ \int w^5 = \frac{432}{35},\ \int w_z^2 = \frac{6}{5}$ we obtain (0.36).

References

1. Doelman A, van der Ploeg H. 2002 Homoclinic stripe patterns. *SIAM Journal on Applied Dynamical Systems* **1**, 65–104.
2. Morgan DS, Kaper TJ. 2004 Axisymmetric ring solutions of the 2D Gray–Scott model and their destabilization into spots. *Physica D: Nonlinear Phenomena* **192**, 33–62.
3. Kolokolnikov T, Ward MJ, Wei J. 2006 Zigzag and Breakup Instabilities of Stripes and Rings in the Two-Dimensional Gray–Scott Model. *Studies in Applied Mathematics* **116**, 35–95.
4. Sewalt L, Doelman A. 2017 Spatially Periodic Multipulse Patterns in a Generalized Klausmeier–Gray–Scott Model. *SIAM Journal on Applied Dynamical Systems* **16**, 1113–1163.
5. Schnakenberg J. 1979 Simple chemical reaction systems with limit cycle behaviour. *Journal of theoretical biology* **81**, 389–400.
6. Iron D, Wei J, Winter M. 2004 Stability analysis of Turing patterns generated by the Schnakenberg model. *Journal of mathematical biology* **49**, 358–390.
7. Ward MJ, Wei J. 2002 The existence and stability of asymmetric spike patterns for the Schnakenberg model. *Studies in Applied Mathematics* **109**, 229–264.
8. Iron D, Ward MJ, Wei J. 2001 The stability of spike solutions to the one-dimensional Gierer–Meinhardt model. *Physica D: Nonlinear Phenomena* **150**, 25–62.
9. Kolokolnikov T, Wei J, Winter M. 2009 Existence and stability analysis of spiky solutions for the Gierer–Meinhardt system with large reaction rates. *Physica D: Nonlinear Phenomena* **238**, 1695–1710.
10. Klausmeier CA. 1999 Regular and irregular patterns in semiarid vegetation. *Science* **284**, 1826–1828.
11. Lejeune O, Tlidi M. 1999 A model for the explanation of vegetation stripes (tiger bush). *Journal of Vegetation science* **10**, 201–208.
12. von Hardenberg J, Meron E, Shachak M, Zarmi Y. 2001 Diversity of vegetation patterns and desertification. *Physical Review Letters* **87**, 198101.
13. Meron E, Gilad E, von Hardenberg J, Shachak M, Zarmi Y. 2004 Vegetation patterns along a rainfall gradient. *Chaos, Solitons & Fractals* **19**, 367–376.
14. Siero E, Doelman A, Eppinga M, Rademacher JD, Rietkerk M, Siteur K. 2015 Striped pattern selection by advective reaction-diffusion systems: Resilience of banded vegetation on slopes. *Chaos: An Interdisciplinary Journal of Nonlinear Science* **25**, 036411.
15. Gowda K, Chen Y, Iams S, Silber M. 2016 Assessing the robustness of spatial pattern sequences in a dryland vegetation model. *Proc. R. Soc. A* **472**, 20150893.
16. Sherratt JA. 2016 When does colonisation of a semi-arid hillslope generate vegetation patterns?. *Journal of mathematical biology* **73**, 199–226.
17. Deblauwe V, Couteron P, Lejeune O, Bogaert J, Barbier N. 2011 Environmental modulation of self-organized periodic vegetation patterns in Sudan. *Ecography* **34**, 990–1001.
18. Deblauwe V, Couteron P, Bogaert J, Barbier N. 2012 Determinants and dynamics of banded vegetation pattern migration in arid climates. *Ecological monographs* **82**, 3–21.
19. Sherratt JA. 2013 Pattern solutions of the Klausmeier model for banded vegetation in semiarid environments IV: Slowly moving patterns and their stability. *SIAM Journal on Applied Mathematics* **73**, 330–350.
20. Doelman A, Kaper TJ, Eckhaus W. 2000 Slowly Modulated Two-Pulse Solutions in the Gray–Scott Model I: Asymptotic Construction and Stability. *SIAM Journal on Applied Mathematics* **61**, 1080–1102.
21. Muratov CB, Osipov V. 2002 Stability of the Static Spike Autosolitons in the Gray–Scott Model. *SIAM Journal on Applied Mathematics* **62**, 1463–1487.

22. Kolokolnikov T, Ward MJ, Wei J. 2005 The existence and stability of spike equilibria in the one-dimensional Gray–Scott model: the pulse-splitting regime. *Physica D: Nonlinear Phenomena* **202**, 258–293.
23. Xie S, Kolokolnikov T. 2017 Moving and jumping spot in a two-dimensional reaction–diffusion model. *Nonlinearity* **30**, 1536.
24. Kolokolnikov T, Sun W, Ward M, Wei J. 2006 The stability of a stripe for the Gierer–Meinhardt model and the effect of saturation. *SIAM Journal on Applied Dynamical Systems* **5**, 313–363.